

University of Nebraska - Lincoln

DigitalCommons@University of Nebraska - Lincoln

Uniformed Services University of the Health
Sciences

U.S. Department of Defense

1994

Regulation of Cellular Ca^{2+} by Yeast Vacuoles

Teresa Dunn

Uniformed Services University of the Health Sciences

Kenneth Gable

Uniformed Services University of the Health Sciences

Troy Beeler

Uniformed Services University of the Health Sciences

Follow this and additional works at: <http://digitalcommons.unl.edu/usuhs>

 Part of the [Medicine and Health Sciences Commons](#)

Dunn, Teresa; Gable, Kenneth; and Beeler, Troy, "Regulation of Cellular Ca^{2+} by Yeast Vacuoles" (1994). *Uniformed Services University of the Health Sciences*. 51.

<http://digitalcommons.unl.edu/usuhs/51>

This Article is brought to you for free and open access by the U.S. Department of Defense at DigitalCommons@University of Nebraska - Lincoln. It has been accepted for inclusion in Uniformed Services University of the Health Sciences by an authorized administrator of DigitalCommons@University of Nebraska - Lincoln.

Regulation of Cellular Ca^{2+} by Yeast Vacuoles*

(Received for publication, June 28, 1993, and in revised form, November 29, 1993)

Teresa Dunn‡, Kenneth Gable, and Troy Beeler

From the Department of Biochemistry, Uniformed Services University of the Health Sciences, Bethesda, Maryland 20814

The role of vacuolar Ca^{2+} transport systems in regulating cellular Ca^{2+} was investigated by measuring the vacuolar Ca^{2+} transport rate, the free energy available to drive vacuolar Ca^{2+} transport, the ability of the vacuole to buffer luminal Ca^{2+} , and the vacuolar Ca^{2+} efflux rate. The magnitude of the Ca^{2+} gradient generated by the vacuolar H^+ gradient best supports a 1 Ca^{2+} :2 H^+ coupling ratio for the vacuolar $\text{Ca}^{2+}/\text{H}^+$ exchanger. This coupling ratio along with a cytosolic Ca^{2+} concentration of 125 nM would give a vacuolar free Ca^{2+} concentration of $\sim 30 \mu\text{M}$. The total vacuolar Ca^{2+} concentration is $\sim 2 \text{mM}$ due to Ca^{2+} binding to vacuolar polyphosphate. The Ca^{2+} efflux rate from the vacuole is less than the growth rate indicating that the steady-state Ca^{2+} loading level of the vacuole is dependent mainly on the Ca^{2+} transport rate and the rate that vacuolar Ca^{2+} is diluted by growth. Based on the kinetic parameters of vacuolar Ca^{2+} accumulation *in vitro*, the maximum rate of Ca^{2+} accumulation *in vivo* is expected to be $\sim 0.2 \text{ nmol of } \text{Ca}^{2+} \text{ min}^{-1} \text{ mg protein}^{-1}$, a rate that is similar to the cellular Ca^{2+} accumulation rate. The cytosolic Ca^{2+} concentration increases from 0.1 μM to 1–2 μM as the extracellular Ca^{2+} concentration is raised from 0.3 mM to 50 mM. The rise in cytosolic Ca^{2+} concentration increases cellular Ca^{2+} from 10 to 300 nM Ca^{2+}/mg by increasing the rate of vacuolar Ca^{2+} accumulation but does not significantly alter the cellular growth rate.

Although Ca^{2+} is believed to be an important regulatory messenger (1, 2) in *Saccharomyces cerevisiae*, little is known about the Ca^{2+} pumps and Ca^{2+} channels which regulate the cytosolic Ca^{2+} concentration. The best-characterized Ca^{2+} transport system in *S. cerevisiae* is the vacuolar $\text{Ca}^{2+}/\text{H}^+$ exchanger (3–6). The importance of vacuolar Ca^{2+} transport in regulating cellular Ca^{2+} is suggested by the observation that mutants defective in the vacuolar H^+ -ATPase (7–10) or in processing of vacuolar proteins (11) have reduced growth rates in 100 mM Ca^{2+} , whereas 100 mM Ca^{2+} has little influence on the wild-type growth rate. Since cytosolic Ca^{2+} concentration is elevated in some of the mutants that have vacuolar defects (8, 12), it could be argued that vacuolar Ca^{2+} transport regulates cytosolic Ca^{2+} . However, it is also possible that the elevated cytosolic Ca^{2+} is an indirect consequence of the vacuolar defect.

The goal of the study presented here is to evaluate the potential role of the vacuole in regulating the cellular Ca^{2+} con-

centration under physiological conditions in wild-type cells grown in media containing both high and low Ca^{2+} concentrations.

EXPERIMENTAL PROCEDURES

Materials—Arsenazo III was obtained from Aldrich. Zymolyase 100T was supplied by Seikagaku Kogyo, Rockville, MD. $^{45}\text{Ca}^{2+}$ was purchased from DuPont-New England Nuclear. All other chemicals were purchased from Sigma.

Yeast Strains/Growth—The yeast strain used in this work was CuH3 (S288C, *MATa his4-619 ura3-52*). Cells were grown according to standard procedures (13). Standard yeast extract bacto-peptone dextran (YPD) and synthetic media were prepared according to Sherman (13). Low phosphate YPD media was made according to the method described by Rubin (14).

Measurement of Ca^{2+} Accumulation by Whole Cells—Two methods were used to measure Ca^{2+} accumulation by cells. In one method, cells were incubated in media containing tracer $^{45}\text{Ca}^{2+}$ (0.1–1 $\mu\text{Ci}/\text{ml}$) for different periods of time, and aliquots were removed, washed three times by centrifugation in YPD medium at 4 °C, and filtered through Millipore HA 0.45- μm filters that were prewashed with 20 mM MgSO_4 . The filters were washed three times with 5 ml of 20 mM MgSO_4 , dried, placed in vials with Beckman Ready Organic™ scintillation mixture, and the amount of Ca^{2+} in the cell was determined by scintillation counting.

In the other method, cells were incubated in media containing 1–100 mM Ca^{2+} for different periods of time and then harvested and washed by centrifugation (4 °C). The cells were resuspended in 0.1 M KCl, 10 mM PIPES, pH 7.0, 0.1 M arsenazo III at a density $10^7/\text{ml}$ (36 °C). Enough digitonin (1 mg/ml) to permeabilize all the cell membranes was added, and the amount of Ca^{2+} released from the cell was determined spectrophotometrically using an SLM-Aminco DW2c dual wavelength spectrophotometer by measuring the increased absorbance caused by the formation of the arsenazo III- Ca^{2+} complex at 660 nm using 685 nm as a reference wavelength. When both methods (filtration and spectrophotometric) were compared under the same experimental conditions, the results were essentially the same.

Isolation of Vacuole Membrane Vesicles—Vacuole membrane vesicles (vesiculated vacuoles) were prepared by the method developed by Anraku and co-workers (3) and stored at $-70 \text{ }^\circ\text{C}$ in 0.1 M potassium glutamate, 10 mM PIPES, pH 7.0, and 10% glycerol.

Permeabilization of Yeast Cells— Ca^{2+} accumulation by intact vacuoles was measured using either osmotically shocked partially regenerated spheroplasts (15) or cells permeabilized by treatment with the detergent digitonin. Treatment of cells with 0.2 mg digitonin/mg protein for 10 min at 26 °C selectively permeabilizes the plasma membrane.

Measurement of Polyphosphate—Polyphosphate was extracted from the cells by the method described by Clark *et al.* (16) and measured by the procedure described by Ames (17).

RESULTS

Effect of Ca^{2+} on the Growth Rate and Ca^{2+} -loading Level of *S. cerevisiae* cells—The role of the vacuole in regulating cellular Ca^{2+} was investigated. Varying the Ca^{2+} concentration in the growth medium from 1 μM to 100 mM has little effect on the growth rate of *S. cerevisiae* cells (18–23). The tolerance of *S. cerevisiae* to high Ca^{2+} concentrations is not due to the inability of Ca^{2+} to enter the cell since the cellular Ca^{2+} increases as the extracellular Ca^{2+} concentration is raised (Fig. 1, inset).

* This work was supported by Grant GM 46495 from the National Institutes of Health and Grants CO71bK and R071AG from the Uniformed Services University of the Health Sciences. The costs of publication of this article were defrayed in part by the payment of page charges. This article must therefore be hereby marked "advertisement" in accordance with 18 U.S.C. Section 1734 solely to indicate this fact.

‡ To whom correspondence should be addressed: Dept. of Biochemistry, Uniformed Services University of the Health Sciences, 4301 Jones Bridge Rd., Bethesda, MD 20814. Tel.: 301-295-3592; Fax: 301-295-3512.

¹ The abbreviations used are: PIPES, 1,4-piperazinebis(ethanesulfonic acid); MES, 4-morpholineethanesulfonic acid.

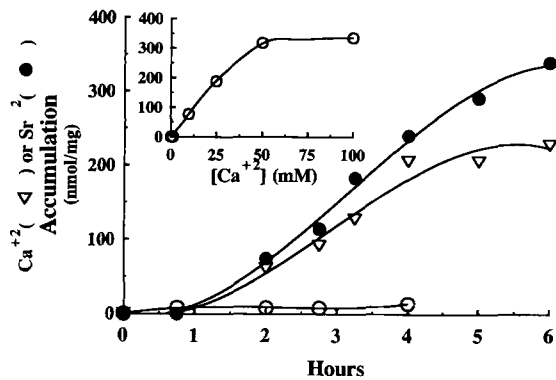


FIG. 1. Accumulation of Ca^{2+} and Sr^{2+} by *S. cerevisiae*. Ca^{2+} (∇) or Sr^{2+} (\bullet) (50 mM) was added (time = 0) to cells ($6 \times 10^6/\text{ml}$) growing in YPD medium at 26 °C. At various times, aliquots were removed, and the amount of Ca^{2+} or Sr^{2+} loading was determined. In a control sample, no Ca^{2+} or Sr^{2+} was added (\circ). To determine Ca^{2+} or Sr^{2+} loading, cells were harvested by centrifugation and washed three times with KCl solution at 4 °C to remove extracellular Ca^{2+} or Sr^{2+} . The cells were then diluted to a concentration of 10^7 cells/ml into a solution containing 0.1 M KCl, 1 mM MgSO_4 , and 100 μM arsenazo III. Intracellular Ca^{2+} or Sr^{2+} was released from the cells by addition of 1 mg/ml digitonin and the absorbance of arsenazo III- Ca^{2+} complex (difference absorbance 660 nm – 685 nm) was measured using an SLM-Aminco DW2c dual wavelength spectrophotometer. *Inset*, the Ca^{2+} -loading level of cells incubated for 5 h in YPD supplemented with the indicated Ca^{2+} concentration was measured as described above.

In normal YPD medium (~ 0.3 mM Ca^{2+}), the cellular Ca^{2+} is 10–20 nmol/mg protein. Addition of 50 mM Ca^{2+} to the YPD growth medium causes a relatively slow increase in the cellular Ca^{2+} to ~ 225 nmol/mg protein after 5 h (Fig. 1) without changing the growth rate.

Ca^{2+} Accumulation by Permeabilized Cells and Vacuolar Membrane Vesicles—The following experiments were designed to determine the relationship between the cytosolic Ca^{2+} concentration and vacuolar Ca^{2+} accumulation. The kinetic and thermodynamic parameters for vacuolar Ca^{2+} transport were investigated.

ATP initiates Ca^{2+} accumulation by isolated vacuole membrane vesicles (4) as well as by permeabilized partially regenerated spheroplasts (Fig. 2). Since nigericin and other proton ionophores inhibit ATP-dependent Ca^{2+} accumulation (4), it was proposed by Ohsumi and Anraku that ATP hydrolysis by the vacuolar H^+ -ATPase establishes a proton gradient that drives Ca^{2+} transport. The Ca^{2+} K_M of the Ca^{2+} transporter in both the isolated vacuole membrane vesicles (data not shown) and permeabilized cells is 25 μM at pH 7.0 and 1 mM Mg^{2+} (Fig. 2B). Permeabilized cells have a maximum Ca^{2+} accumulation rate (V_{max}) of 35 nmol of $\text{Ca}^{2+} \text{ min}^{-1} (\text{mg cell protein})^{-1}$ (Fig. 2B). Therefore, the vacuolar Ca^{2+} accumulation rate in the presence of 125 nM Ca^{2+} is expected to be ~ 0.2 nmol $\text{Ca}^{2+} \text{ min}^{-1} (\text{mg cell protein})^{-1}$ which is comparable to the rate of whole cell Ca^{2+} accumulation in YPD medium (0.1 – 0.2 nmol $\text{Ca}^{2+} \text{ min}^{-1} (\text{mg cell protein})^{-1}$). Thus, the overall rate of cellular Ca^{2+} accumulation could depend on the rate of vacuolar Ca^{2+} accumulation and not on the rate of Ca^{2+} influx across the plasma membrane.

Effect of the Proton Gradient on Ca^{2+} Accumulation by Vacuole Membrane Vesicles—To determine if ATP is required directly by the Ca^{2+} transport system, H^+ gradients across the yeast vacuolar membrane were formed in the absence of ATP by diluting K^+ -equilibrated vacuolar membrane vesicles into solutions containing differing ratios of Tris^+ and K^+ , and the ionophore, nigericin. Nigericin mediates the exchange of one proton for one K^+ causing the formation of a H^+ gradient which is expected to equal the K^+ gradient. Ca^{2+} accumulation was

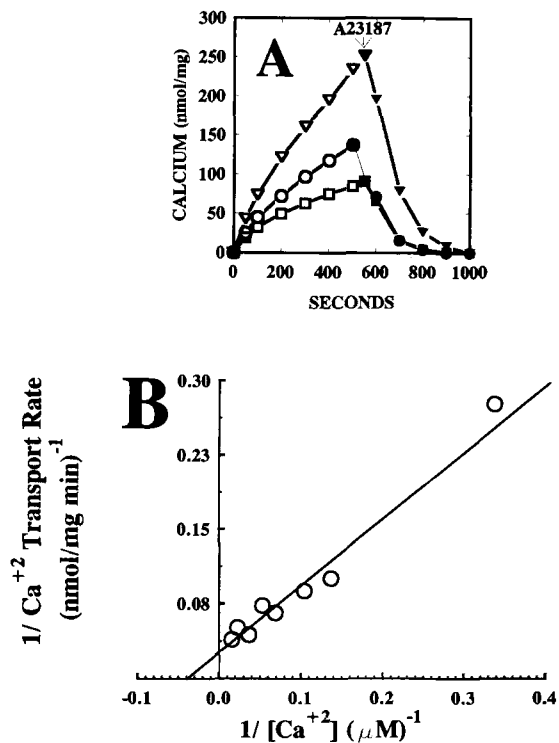


FIG. 2. Kinetic analysis of Ca^{2+} accumulation by permeabilized partially regenerated spheroplasts. *Panel A*, partially regenerated spheroplasts (2.8 mg/ml protein) were prepared as described under "Experimental Procedures" and resuspended in KCl solution containing 0.6 M sorbitol. A 40-fold dilution of the partially regenerated spheroplasts into 0.1 M KCl, 10 mM PIPES, pH 7.0, 50 μM arsenazo III, 1.5 mM MgSO_4 , and either 100 μM (∇), 25 μM (\circ), or 6.3 μM (\square) CaCl_2 (27 °C) causes an osmotic shock which permeabilizes the plasma membrane without causing lysis or irreversible damage to the internal membranes. Ca^{2+} accumulation was initiated by the addition of 1 mM ATP 100 s after cell dilution. Ca^{2+} uptake was monitored spectrophotometrically by measuring the decrease in the absorbance of the arsenazo III- Ca^{2+} complex at 660 nm using 685 nm as a reference wavelength. At the end of each measurement the accumulated Ca^{2+} was released by the addition of 5 μM A23187 (closed symbols). The absorbance change was calibrated by titration of the arsenazo III with both Ca^{2+} and EGTA. *Panel B*, Double-reciprocal plot ($1/v$ versus $1/[S]$) of the data in *panel A*.

measured spectrophotometrically using the Ca^{2+} indicator arsenazo III. As shown in Fig. 3A, the rate of Ca^{2+} accumulation by vacuole membrane vesicles is dependent on the K^+ gradient (and therefore on the H^+ gradient). No Ca^{2+} accumulation is observed in the absence of nigericin or when nigericin is replaced with the K^+ ionophore, valinomycin, demonstrating that neither a K^+ gradient nor K^+ diffusion potential (inside-negative) drives Ca^{2+} transport. An apparent H^+ K_m of 2 μM is determined from the relationship between the K^+ gradient and the Ca^{2+} transport rate (Fig. 3B).

The $\text{Ca}^{2+}/\text{H}^+$ Exchanger Coupling Ratio—To determine the stoichiometry of the $\text{Ca}^{2+}/\text{H}^+$ -exchanger, the free intravesicular Ca^{2+} concentration established by the proton gradient generated by the vacuolar H^+ -ATPase was determined. Vesicles were equilibrated with different concentrations of $\text{Ca}^{2+} + ^{45}\text{Ca}^{2+}$, and the amount of Ca^{2+} trapped within the vesicles was measured by filtration (Fig. 4A). The trapped vesicular Ca^{2+} can be divided into a component that is directly proportional to the Ca^{2+} concentration and another that saturates. The component that increases linearly with the Ca^{2+} concentration represents free vesicular Ca^{2+} . The trapped volume of vacuole membrane vesicles is calculated to be 2.4 $\mu\text{l}/\text{mg}$ protein, a value similar to that of other biomembrane vesicles. The saturable component probably represents Ca^{2+} binding to residual polyphosphate in the vesicle lumen (24).

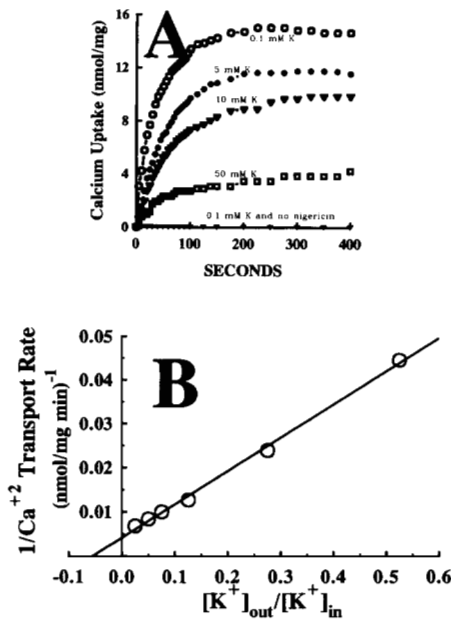


FIG. 3. Relationship between Ca²⁺ accumulation by vacuole membrane vesicles and the H⁺ gradient formed by K⁺/H⁺ exchange. Panel A, vacuolar membrane vesicles (6.5 mg/ml protein, equilibrated in 0.1 M K-HEPES) are diluted 100-fold into solutions containing different ratios of 0.1 M Tris-HEPES and 0.1 M K-HEPES ([K⁺] indicated in figure) along with 1 mM MgSO₄, 50 μM arsenazo III, 50 μM CaCl₂, and 1 μM nigericin. In a control series (▼), nigericin was left out of the assay solution. Ca²⁺ accumulation was monitored by measuring the change in arsenazo III absorbance associated with the Ca²⁺-arsenazo III complex (660 nm using 685 nm as a reference wavelength). Panel B, double-reciprocal plot of (Ca²⁺ uptake rate)⁻¹ versus the (K⁺ gradient)⁻¹.

Since vesicles passively equilibrated with 12 mM Ca²⁺ (Fig. 4A) sequester the same amount of Ca²⁺ as vesicles actively loaded in the presence of 0.1 mM Ca²⁺ (Fig. 4B), a 120-fold Ca²⁺ gradient (0.1 mM Ca²⁺ outside, 12 mM Ca²⁺ inside) is formed by H⁺/Ca²⁺ exchange under conditions where the H⁺ gradient generated by the H⁺-ATPase is ~15-fold (24). An electroneutral coupling ratio of 2 H⁺:1 Ca²⁺ can account for the observed Ca²⁺ gradient since this coupling ratio has the potential to form a 225-fold Ca²⁺ gradient ($([H^+]_{in}/[H^+]_{out})^2 = 15^2$). Assuming no membrane potential, a 1H⁺:1Ca²⁺ and a 3H⁺:1Ca²⁺ coupling ratio could form a 15- and a 3375-fold Ca²⁺ gradient, respectively.

A 225-fold Ca²⁺ gradient across the vacuolar membrane *in vivo* would predict a free vacuolar Ca²⁺ concentration of about 30 μM for cells growing in YPD. Since the total Ca²⁺ concentration in the vacuole is estimated to be 2–4 mM, most of the vacuolar Ca²⁺ must be bound.

Effect of Vacuolar Polyphosphate on Ca²⁺ Uptake by *S. cerevisiae*—Since yeast vacuoles contain large amounts of polyphosphate that range in size from 3 to 260 units with most being 7 to 20 units (25), the role of polyphosphate in vacuolar Ca²⁺ sequestration was investigated. The strain used in this study accumulates ~0.1 mg polyphosphate/mg protein when grown in YPD medium. Ca²⁺ binding to polyphosphate was investigated using several experimental approaches. First, properties of Ca²⁺ binding to synthetic polyphosphate were determined. Next, Ca²⁺ binding to cellular polyphosphate was compared with that of synthetic polyphosphate. Finally, the effect of the vacuolar polyphosphate content on Ca²⁺ accumulation by whole cells and by cells with the plasma membrane permeabilized was determined.

The affinity and capacity of polyphosphate to bind Ca²⁺ was determined spectrophotometrically using the Ca²⁺-indicator

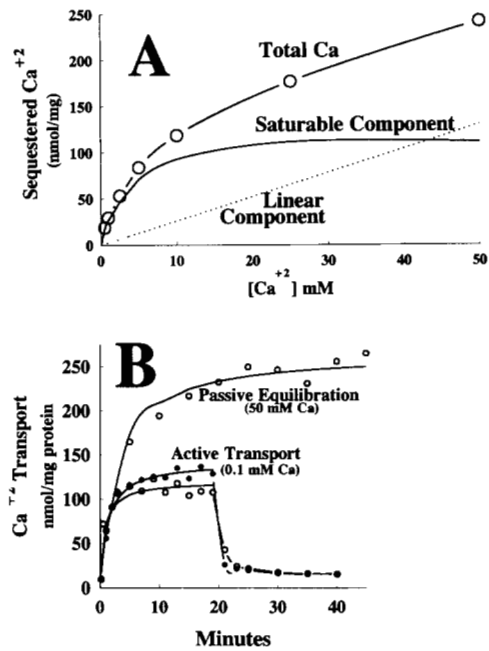


FIG. 4. Determining the intravesicular Ca²⁺ concentration during Ca²⁺ uptake by vacuole membrane vesicles. Panel A, vesicles were incubated in 0.1 M KCl, 1 mM MgSO₄, 10 mM PIPES, pH 7.0, and the indicated CaCl₂ concentration along with 1 μCi/ml ⁴⁵Ca²⁺. After a 30-min incubation, the vesicles were filtered, and the amount of Ca²⁺ in the vesicles was determined (○). Ca²⁺ sequestration appears to be the sum of two Ca²⁺ pools, a saturable pool (solid line) and a pool that is directly proportional to the external Ca²⁺ concentration (....). Panel B, comparison of the passive Ca²⁺ influx rate with the rate of Ca²⁺/H⁺ exchange. The Ca²⁺ uptake solution contained 0.1 M KCl, 1 mM MgSO₄, 10 mM PIPES, pH 7.0, and either 50 mM Ca²⁺ + 50 μCi/ml ⁴⁵Ca²⁺ (to measure passive Ca²⁺ influx), or 0.1 mM Ca²⁺ + 0.1 μCi/ml ⁴⁵Ca²⁺ + 1.0 mM MgATP (to measure active Ca²⁺ accumulation). Ca²⁺ accumulation was initiated by the addition of 1.4 mg protein/ml (passive Ca²⁺ influx) or 0.04 mg protein/ml (active transport) vacuole membrane vesicles. At different times 1-ml aliquots were removed and filtered on Millipore HA 0.45-μm filters that were prewashed with 20 mM MgSO₄. The filters were washed three times with 5 ml of 20 mM MgSO₄, dried, and counted to determine the trapped ⁴⁵Ca²⁺. Active Ca²⁺ transport by two different vacuole membrane vesicle preparations is shown.

arsenazo III. The free Ca²⁺ concentration in the presence of 80 μg/ml polyphosphate was measured as the total Ca²⁺ concentration was varied (Fig. 5).

Synthetic polyphosphates containing averages of 5, 18, and 31 phosphate residues were used. At pH 6.0 (close to the vacuolar pH *in vivo* (26,27)), the Ca²⁺ dissociation constant is 6–8 μM (Fig. 5). The 31-residue polyphosphate binds 1 Ca²⁺/2.5 phosphate residues with high affinity suggesting that, except for the 3 phosphate residues on each end, the high affinity Ca²⁺-binding site is formed by 2 phosphate residues. The binding of Ca²⁺ does not change significantly when the pH is decreased to 5.7 or increased to 6.8 (data not shown); however, Mg²⁺ is a strong competitor for Ca²⁺ binding (Fig. 5). In the presence of 1 mM Mg²⁺, the dissociation constant is increased to ~1 mM. The data indicate that Mg²⁺ and Ca²⁺ bind to polyphosphate with similar affinities.

Treatment of yeast cells with high detergent concentrations exposes intracellular high affinity Ca²⁺-binding sites (Fig. 6). The detergent-exposed latent Ca²⁺ binding activity of *S. cerevisiae* can be primarily attributed to polyphosphate for the following reasons. 1) Latent Ca²⁺ binding activity is directly proportional to the polyphosphate content of the cells which varies with the phosphate concentration (0.01–1 mM) of the growth media. 2) The Ca²⁺/phosphate residue stoichiometry (0.4 Ca²⁺/phosphate residue in 50 μM Ca²⁺) of the latent Ca²⁺ binding is

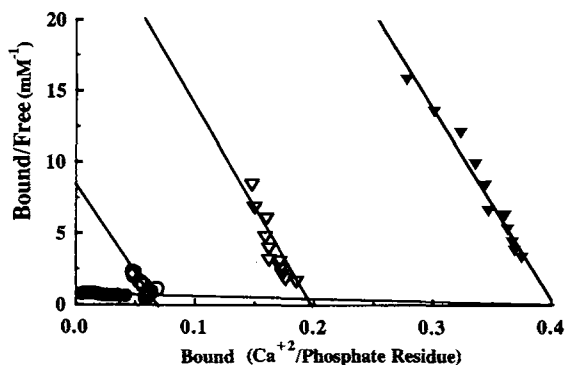


FIG. 5. Scatchard plots of Ca^{2+} -binding to polyphosphate. The assay solution contained 0.1 M KCl, 10 mM MES, pH 6.0, 20 μM arsenazo III and polyphosphate (0.8 mM phosphate residue) of average lengths 5 (\circ), 18 (∇), or 31 (\blacktriangledown) phosphate residues. Ca^{2+} binding to polyphosphate was calculated by subtracting the Ca^{2+} bound to arsenazo III and the free Ca^{2+} from the total Ca^{2+} . Arsenazo III-bound Ca^{2+} was calculated from the ratio of absorbance change at 660 nm to the maximum absorbance change observed for saturated arsenazo III. Free Ca^{2+} was determined from a calibration curve of the absorbance at 660 nm versus free Ca^{2+} (free Ca^{2+} = total Ca^{2+} minus Arsenazo III-bound Ca^{2+}) measured in the absence of polyphosphate. The effect of 1 mM Mg^{2+} on Ca^{2+} binding to the 31-mer is also shown (\bullet).

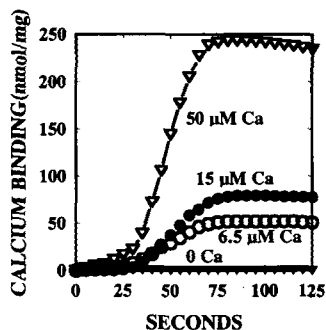


FIG. 6. Ca^{2+} binding to intracellular sites following the addition of the detergent digitonin. *S. cerevisiae* cells were suspended in 0.1 M KCl, 10 mM PIPES, 20 μM arsenazo III, pH 7.0, containing the indicated Ca^{2+} concentration. At time = 0, 1 mg/ml digitonin was added to permeabilize all the cellular membranes to permit exposure of intracellular Ca^{2+} . The kinetics of permeabilization and Ca^{2+} binding are shown. The binding of Ca^{2+} to the detergent-exposed intracellular sites was determined by measuring the change in the difference absorbance of the arsenazo III- Ca^{2+} complex at 660 nm using 685 as a reference wavelength.

the same as is observed for synthetic polyphosphate containing more than 30 phosphate residues. 3) The effect of pH and Mg^{2+} on the latent Ca^{2+} binding activity is the same as is observed for synthetic polyphosphate.

Based on the affinity and stoichiometry of Ca^{2+} binding to polyphosphate and assuming a free Mg^{2+} concentration of 1 mM, vacuolar polyphosphate is expected to have the capacity to bind about 100 mM Ca^{2+} with a dissociation constant of about 1 mM. The Ca^{2+} loading level of cells grown in YPD (about 0.3 mM Ca^{2+}) is about 10 nmol/mg cell protein giving a total vacuolar Ca^{2+} concentration of 2–4 mM, indicating that only about 3% of the vacuolar polyphosphate-binding sites are occupied with Ca^{2+} . A free vacuolar Ca^{2+} concentration of only 30 μM would give a bound Ca^{2+} concentration of 3 mM.

The effect of the cellular polyphosphate content on Ca^{2+} uptake was determined both *in vitro* (Fig. 7A) and *in vivo* (Fig. 7B). The *in vitro* measurements were performed using cells in which the plasma membrane was permeabilized by digitonin treatment which preserves vacuolar polyphosphate. The polyphosphate content of the vacuoles was varied by incubating cells in phosphate-free YPD for various times. ATP-dependent

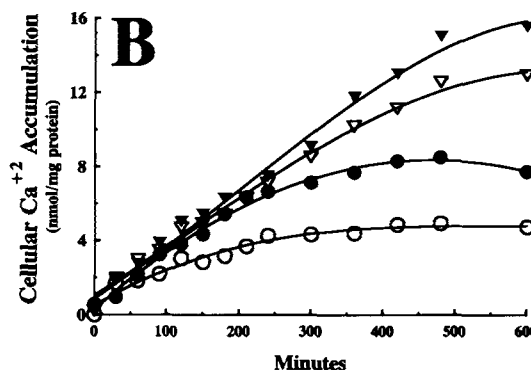
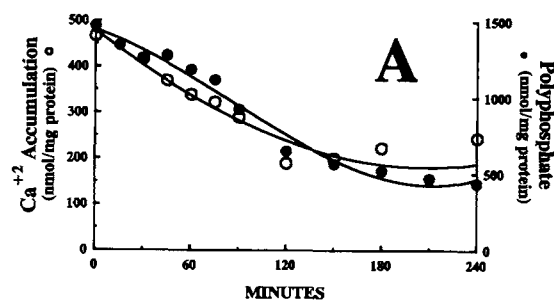


FIG. 7. Effect of cellular polyphosphate on Ca^{2+} accumulation by permeabilized cells. Panel A, cells, grown to a density of 1.2×10^7 in YPD, were transferred into phosphate-free YPD medium and at various times, aliquots were removed and the polyphosphate content and capacity for ATP-dependent Ca^{2+} uptake of the permeabilized cells were determined. Panel B, relationship between cellular content of Ca^{2+} and polyphosphate. Cells were grown to an OD_{600} of 0.4 at 26 $^{\circ}\text{C}$ in modified SD medium containing 100 μM phosphate, 300 μM CaCl_2 , and 100 μM MgSO_4 . The cells were diluted to an OD_{600} of 0.1 in media containing 25 (\circ), 125 (\bullet), 250 (∇) or 500 (\blacktriangledown) μM phosphate and incubated for 3.5 h. $^{45}\text{Ca}^{2+}$ (1 $\mu\text{Ci}/\text{ml}$) was then added ($t = 0$) and at the indicated times 1-ml aliquots were removed, filtered, and the filters were washed four times with 5 ml of cold 20 mM MgSO_4 . Aliquots were also removed for polyphosphate determination; the polyphosphate content continuously changes during the time course of Ca^{2+} loading due to the accumulation and metabolism of the phosphate by the cells (which did not depend on Ca^{2+}). The polyphosphate content at 420 min was 1.1, 2.4, 3.7, and 5.9 μmol of phosphate residue/mg protein for cells placed in 25, 125, 250, and 500 μM phosphate, respectively.

Ca^{2+} accumulation by permeabilized cells was proportional to their polyphosphate content (Fig. 7A). The ratio of Ca^{2+} accumulated/phosphate residue was ~ 0.3 . The Ca^{2+} -loading capacity of permeabilized cells (470 nmol Ca^{2+}/mg) is ~ 47 times greater than the Ca^{2+} -loading level *in vivo* reflecting the difference in the cytosolic Ca^{2+} concentration *in vivo* (0.1–0.2 μM) and the Ca^{2+} concentration in the assay medium (~ 27 μM free Ca^{2+}).

The role of polyphosphate in sequestering cellular Ca^{2+} is further demonstrated by measuring the effect of cellular polyphosphate levels on the *in vivo* Ca^{2+} content (Fig. 7B). The amount of cellular Ca^{2+} increases with increasing cellular polyphosphate. The ratio of cellular Ca^{2+} to polyphosphate residues remains constant at about 0.003, once again demonstrating that the *in vivo* vacuolar Ca^{2+} level for cells grown in 0.3 mM Ca^{2+} is ~ 100 times lower than the level of polyphosphate Ca^{2+} -binding sites. The Ca^{2+} content of cells growing in 50 mM Ca^{2+} is also proportional to cellular polyphosphate content; however, the ratio of Ca^{2+} to polyphosphate residues increases to ~ 0.2 (data not shown).

Vacuolar Ca^{2+} Efflux—The above data indicate that the rate-limiting step of Ca^{2+} accumulation by *S. cerevisiae* cells is vacuolar transport and that polyphosphate acts as a Ca^{2+} sink within the vacuole lumen. The next question that was addressed was whether Ca^{2+} sequestration in the vesicles was

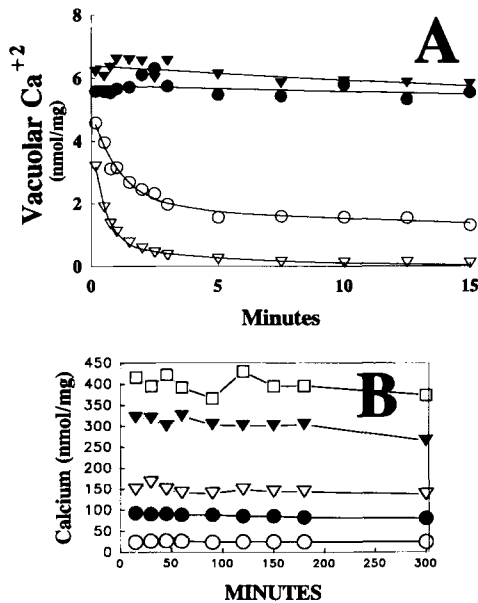


FIG. 8. Rate of Ca²⁺ release from vacuoles of permeabilized cells (A) and from whole cells (B). Panel A, partially regenerated spheroplasts (1 mg/ml) were diluted into 0.05 M KCl, 25 μM (10 μCi/ml ⁴⁵Ca²⁺) to permeabilize the cells by osmotic shock and to equilibrate the Ca²⁺ across the vacuole membrane. KCl and sorbitol were then added to give a final concentration of 0.1 M KCl, 0.3 M sorbitol, 10 mM PIPES, pH 7.0, and 25 μM Ca²⁺. The permeabilized partially regenerated spheroplasts were diluted 100-fold into KCl solution containing 1 mM EGTA (●), 50 μM CaSO₄ (○), 1 mM LaCl₃ + 50 μM CaSO₄ (▼) or 1 μM A23187 (▽). At various times, aliquots were removed and amount of ⁴⁵Ca²⁺ remaining in the cell determined by filtration. Panel B, cells were grown at 27°C in YPD containing either 0.3 (○), 1 (●), 3 (▽), 10 (▼), or 30 (□) mM Ca²⁺ and 1 μCi/ml ⁴⁵Ca²⁺ until they reached a density of about 10⁷/ml. The cells were harvested by centrifugation, washed three times, and diluted into YPD (about 0.3 mM Ca²⁺) without ⁴⁵Ca²⁺. At the indicated times, 5-ml aliquots were removed and passed through Millipore HA 0.45-μm filters that were prewashed with 20 mM MgSO₄. The filters were washed three times with 5 ml of 20 mM MgSO₄ to remove extracellular ⁴⁵Ca²⁺, dried, and the cell-associated ⁴⁵Ca²⁺ determined by scintillation counting.

reversible. The rate of Ca²⁺ efflux from yeast vacuoles was measured both *in vitro* and *in vivo*. Permeabilized cells equilibrated with 25 μM Ca²⁺ sequester ~6 nmol Ca²⁺/mg protein (about 0.14 nmol/mg would be free, most of the rest is bound to polyphosphate) (Fig. 8). This observation further supports the conclusion that the free vacuole Ca²⁺ concentration *in vivo* is ~30 μM since cells accumulate 10–20 nmol Ca²⁺/mg protein. The rate of Ca²⁺ efflux from the vacuole of permeabilized cells was measured following dilution into an EGTA solution. The Ca²⁺ efflux rate was only 0.016 nmol Ca²⁺ min⁻¹ (mg protein)⁻¹; therefore, the half-time for Ca²⁺ release from the vacuole exceeds the doubling time for cells under normal growth conditions. ⁴⁵Ca²⁺ release was observed when unlabeled Ca²⁺ was added to the dilution medium, but this is due to ⁴⁵Ca²⁺-Ca²⁺ exchange mediated by the Ca²⁺/H⁺ exchanger since in parallel experiments it was observed that extracellular ⁴⁵Ca²⁺ was accumulated by vacuoles in exchange with luminal unlabeled Ca²⁺.

The Ca²⁺ ionophore, A23187, was able to induce the release of all sequestered Ca²⁺ in the absence of extracellular Ca²⁺. Like the intrinsic Ca²⁺/2H⁺ exchanger, A23187 mediates the transmembrane exchange of one Ca²⁺ for two protons. Perhaps the reason that the intrinsic exchanger fails to release Ca²⁺ from the vacuole lumen while A23187 does is that A23187 has a relatively high affinity for protons (high pK) so that it transports protons in both directions, while the intrinsic exchanger may have a low affinity for protons (low pK) on the cytosolic

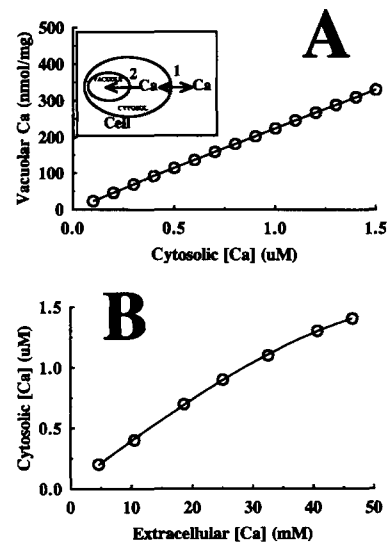


FIG. 9. Model for Ca²⁺ metabolism by *S. cerevisiae* cells. Panel A, the predicted steady-state vacuolar Ca²⁺ is plotted as a function of the cytosolic Ca²⁺ concentration. The model used to predict the steady-state vacuolar Ca²⁺ (inset) assumes that vacuolar Ca²⁺ transport rate is given by the Michaelis-Menten equation, and that vacuolar Ca²⁺ efflux is essentially zero so that steady-state is reached when the vacuolar Ca²⁺ transport rate (reaction 2) is equal to the rate that vacuolar Ca²⁺ is diluted by cell growth. Panel B, The cytosolic Ca²⁺ concentration that is predicted to give the experimentally observed cellular Ca²⁺ content (Fig. 1) is plotted against the extracellular Ca²⁺ concentration.

side blocking the exchange of cytosolic protons with luminal Ca²⁺.

To compare the rate of Ca²⁺ efflux from whole cells with that of permeabilized cells, cells were grown for several generations in YPD medium containing a variety of Ca²⁺ concentrations with ⁴⁵Ca²⁺ and then shifted to YPD medium without ⁴⁵Ca²⁺. The ⁴⁵Ca²⁺ efflux rate was measured by filtration. As is seen in Fig. 8B, most of the cellular Ca²⁺ is in a stable nonreleaseable pool, and the amount of Ca²⁺ in this stable pool increases with increasing extracellular Ca²⁺ concentration. This experiment indicates that the *in vivo* vacuolar Ca²⁺ efflux rate is also very low.

DISCUSSION

Model of Ca²⁺ Metabolism by *S. cerevisiae*—A model for Ca²⁺ metabolism by *S. cerevisiae* cells is presented in the inset of Fig. 9. Steady-state Ca²⁺ gradients across the plasma membrane are rapidly established (within seconds) following changes in the extracellular Ca²⁺ concentration. The mechanisms by which Ca²⁺ enters the cell and is actively pumped out are not known, but a 25,000-fold Ca²⁺ gradient across the plasma membrane can apparently be maintained. The rate of Ca²⁺ accumulation by the vacuole (the major Ca²⁺-sequestering organelle) is dependent on the rate of Ca²⁺ transport mediated by the Ca²⁺/2H⁺ exchanger and the cell growth rate. The vacuolar Ca²⁺ uptake rate is predicted to increase linearly with the cytosolic Ca²⁺ concentration because of the relatively high K_M (25 μM) and the high Ca²⁺ binding capacity of the vacuolar lumen (~400 nmol Ca²⁺/mg protein). Because most of the cellular Ca²⁺ is found in the vacuole, the rate of cellular Ca²⁺ accumulation is dependent on the rate of vacuolar Ca²⁺ accumulation. Because the vacuolar Ca²⁺ efflux rate is less than the growth rate, the steady-state vacuolar Ca²⁺ level is reached when the rate of vacuolar Ca²⁺ transport is equal to the rate of vacuolar Ca²⁺ dilution by growth. The rate of vacuolar Ca²⁺ dilution through growth would be k_{growth} × [Ca]_{vacuolar} where k_{growth} is the rate constant for cell growth and [Ca]_{vacuolar} is the

total vacuolar Ca^{2+} content. If vacuolar Ca^{2+} transport follows Michaelis-Menten kinetics, $v = V_{\max}[\text{Ca}^{2+}]_{\text{cytosol}}/([\text{Ca}^{2+}]_{\text{cytosol}} + K_M)$, the steady-state vacuolar Ca^{2+} content would be $V_{\max}[\text{Ca}^{2+}]_{\text{cytosol}}/([\text{Ca}^{2+}]_{\text{cytosol}} + K_M)k_{\text{growth}}$. Based on the kinetic parameters ($V_{\max} = 35 \text{ nmol Ca}^{2+} \text{ min}^{-1} (\text{mg protein})^{-1}$; $K_M = 25 \mu\text{M}$) determined from permeabilized cells, and a growth rate of $6 \times 10^{-3} \text{ min}^{-1}$, the total vacuolar Ca^{2+} content is predicted to be directly proportional to the cytosolic Ca^{2+} concentration ($233[\text{Ca}^{2+}]_{\text{cytosol}} \text{ nmol } (\mu\text{M mg protein})$) (Fig. 9A). According to the proposed model, the cytosolic Ca^{2+} concentrations that would give the observed cellular Ca^{2+} levels of 10–300 nmol $\text{Ca}^{2+}/\text{mg protein}$ would be 0.1–1.4 $\mu\text{M Ca}^{2+}$, meaning the cytosolic Ca^{2+} would have to increase from 0.1 to 1.4 μM as the extracellular Ca^{2+} increases from 0.3 to 100 mM (Fig. 9B).

Addition of 100 mM Ca^{2+} to the growth medium has no significant effect on the growth rate suggesting that increasing the cytosolic Ca^{2+} concentration to 1–2 μM does not alter the cellular physiology of exponentially growing yeast cells. In this regard, it is interesting that at these cytosolic Ca^{2+} concentrations, calmodulin would be expected to be activated by Ca^{2+} and yet there is no influence on cell growth. These results complement the findings of Geiser *et al.* (28) which demonstrate that, while calmodulin is required for growth, Ca^{2+} binding to calmodulin is apparently not required. Taken together these results indicate that Ca^{2+} binding to calmodulin does not affect vegetative cell growth.

REFERENCES

- Davis, T. N., Urdea, M. S., Masiarz, F. R., and Thorner, J. (1986) *Cell* **47**, 423–431
- Iida, H., Yagawa, Y., and Anraku, Y. (1990) *J. Biol. Chem.* **265**, 13391–13399
- Kakinuma, Y., Ohsumi, Y., and Anraku, Y. (1981) *J. Biol. Chem.* **256**, 10859–10863
- Ohsumi, Y., and Anraku, Y. (1983) *J. Biol. Chem.* **258**, 5614–5617
- Okorokov, L. A., Kulakovskaya, T. V., Lichko, L. P., and Polorotova, E. V. (1985) *FEBS Lett.* **192**, 303–306
- Uchida, E., Ohsumi, Y., and Anraku, Y. (1985) *J. Biol. Chem.* **260**, 1090–1095
- Ohya, Y., Ohsumi, Y., and Anraku, Y. (1986) *J. Gen. Microbiol.* **132**, 979–988
- Ohya, Y., Umemoto, N., Tanida, I., Ohta, A., Iida, H., and Anraku, Y. (1991) *J. Biol. Chem.* **266**, 13971–13977
- Shih, C.-K., Wagner, R., Feinstein, S., Kanik-Ennulat, C., and Neff, N. (1988) *Mol. Cell. Biol.* **8**, 3094–3103
- Hirata, R., Ohsumi, Y., Nakano, A., Kawasaki, H., Suzuki, K., and Anraku, Y. (1990) *J. Biol. Chem.* **265**, 6726–6733
- Kitamoto, K., Yoshizawa, K., Ohsumi, Y., and Anraku, Y. (1988) *J. Bacteriol.* **170**, 2687–2691
- Halachmi, D., and Eilam, Y. (1993) *FEBS Lett.* **316**, 73–78
- Sherman, F. (1991) *Methods Enzymol.* **194**, 3–21
- Rubin, G. M. (1973) *J. Biol. Chem.* **248**, 3860–3875
- Novick, P., Osmond, B., and Botstein, D. (1989) *Genetics* **121**, 659–674
- Clark, J. E., Beegen, H., and Wood, H. G. (1986) *J. Bacteriol.* **168**, 1212–1219
- Ames, B. N. (1966) *Methods Enzymol.* **8**, 115–118
- Carafoli, E., Balcavage, W. X., Lehninger, A. L., and Mattoon, J. R. (1970) *Biochim. Biophys. Acta* **205**, 18–26
- Davis, T. N., and Thorner, J. (1986) in *Yeast Cell Biology* (Hicks, J., ed) pp. 477–503, Alan R. Liss, New York
- Lomander, L. (1965) *Physiol. Plant* **18**, 153–158
- Lomander, L. (1965) *Physiol. Plant* **18**, 968–975
- Morris, E. O. (1958) in *The Chemistry and Biology of Yeast* (Cook, A. H., ed) pp. 251–321, Academic Press, New York
- Olson, B. H., and Johnson, M. J. (1949) *J. Bacteriol.* **57**, 235–246
- Ohsumi, Y., and Anraku, Y. (1981) *J. Biol. Chem.* **256**, 2079–2082
- Urech, K., Durr, M., Boller, T., Wiemken, A., and Schwencke, J. (1978) *Arch. Microbiol.* **116**, 275–278
- Navon, G., Shulman, R. G., Yamane, T., Eccleshall, T. R., Lam, K. B., Baronofsky, J. J., and Marmor, J. (1979) *Biochemistry* **18**, 4487–4499
- Nicolay, K., Scheffers, W. A., Bruinenberg, P. M., and Kaptein, R. (1982) *Arch. Microbiol.* **133**, 83–89
- Geiser, J. R., van Tuinen, D., Brockerhoff, S. E., Neff, M. N., and Davis, T. N. (1991) *Cell* **65**, 949–959